



## Original Research Article

### Kinetics and Equilibrium Studies on Silica Supported Al-Zn Bimetals as Adsorbent for the Removal of Methylene Blue and Malachite Green Dyes from Aqueous Solution

**\*Samaila, M.B., Aminu, A. and Lukman, O.A.**

Department of Pure and Industrial Chemistry, Umaru Musa Yar'adua University, PMB 2218, Katsina, Katsina State, Nigeria

\*samaila.muazu@umyu.edu.ng

#### ARTICLE INFORMATION

##### Article history:

Received 29 Aug, 2019

Revised 02 Dec, 2019

Accepted 04 Dec, 2019

Available online 30 Dec, 2019

##### Keywords:

Bimetals

Adsorbents

Methylene blue

Malachite green

Millet husk

#### ABSTRACT

*Silica supported Al/Zn bimetal has been prepared successfully using millet husk ash and was subsequently used as adsorbent to remove methylene blue and malachite green from aqueous solution by batch adsorption technique. The material displayed very good adsorption properties that are consistent with some of the viable adsorbents reported in the literature. The amounts adsorbed in percentage at maximum concentration of 50 mg/L are 98.75% and 88.81% for methylene blue and malachite green respectively. The adsorption process followed pseudo-second order kinetics and interestingly, the adsorption data fitted both Langmuir and Freundlich models. Surprisingly, the prepared silica supported Al/Zn bimetal adsorbent has higher adsorption capacities for methylene blue than malachite green. Therefore, this material could be used as a cost-effective adsorbent in wastewater/effluents treatment.*

© 2019 RJEES. All rights reserved.

## 1. INTRODUCTION

Industrial effluent containing dyes pose threat to the environment. The colour in water affects the nature of water, and it interferes with the normal biological activities of aquatic life (Ponnusami *et al.*, 2010). Some of the dyes cause rapid depletion of dissolved oxygen affecting aquatic life adversely. Some of the dyes are toxic and carcinogenic and most of them have been shown to cause allergy, dermatitis, skin irritation and intestinal cancer to humans (Chatterjee *et al.*, 2007). Without adequate treatment, these dyes are persistent in the environment and hence pose serious threat to survival of both terrestrial and aquatic ecosystem (Carneiro *et al.*, 2010).

A wide range of various treatment methods namely, ion exchange, biodegradation, oxidation, solvent extraction and adsorption have been reported to be used for removal of organic pollutants from industrial effluents (Das and Subramanyam, 2009)

Many physicochemical methods available for the removal of colour are either costly or inefficient (Khaled *et al.*, 2009). Among them adsorption is proven to be one of the most efficient techniques (Khaled *et al.*, 2009). However, as cost of conventional adsorbents is too high, it is necessary to search for low cost adsorbents.

Millet husk (Figure 1) is one of the common agricultural wastes. Agricultural wastes, such as wood, herbaceous plants, crops and forest residues, as well as animal wastes are potentially huge source of energy. In Nigeria, large quantities of these wastes are generated annually and are vastly under utilized. Studies have shown that these agricultural residues could be processed into useful products (Solfes, 2000). The advantage of using waste materials as an adsorbent is that, it also helps in the management of waste, thus solving environmental problems. Waste materials have been used either in their raw form or after some physical or chemical modification and have been shown to have great potential for the removal of heavy metal ions and organics from aqueous solution (Kurniawan *et al.*, 2009).

Millet husk ash (MHA) is a byproduct from burning of millet husk after processing using a control burning method. Millet husk ash consist of 73.1% SiO<sub>2</sub>, 0.025% Al<sub>2</sub>O<sub>3</sub>, 4.2% Fe<sub>2</sub>O<sub>3</sub>, 10.5% CaO, 0.04% MgO, 7.5% K<sub>2</sub>O, 1.61% P<sub>2</sub>O<sub>5</sub>, 0.44% MnO, 1.4% SO<sub>3</sub> and 11.04% percentage by weight (Jimoh *et al.*, 2013).

The aim of this research was to develop an adsorbent from cheap and readily available material and apply such material in waste water purification.



Figure 1: Image of millet husk.

## 2. MATERIALS AND METHODS

### 2.1. Materials

The materials and chemicals used in this study include laboratory oven (MINO/100/F), shaker (SFI flask shaker), UV/Vis Spectrophotometer (T60, PG Instruments), centrifuge (K240), FTIR spectrophotometer (VERTEX 70/70v, Agilent Technologies), scanning electron microscope (Phenom 800-07334), hot plate (1103, JENWAY), NaOH (Querec) and HNO<sub>3</sub> (Querec).

### 2.2. Preparation of Adsorbent

The millet husk was washed several times with water, rinsed with distilled water and dried at room temperature for 24 hrs. 100 g of the dried sample was soaked in 1 L of 1.0 M nitric acid at room temperature for 24 hrs. It was then washed with distilled water until a constant pH and then dried in an oven at 110 °C

for 24 hrs. The dried sample was calcined at 600 °C for 6 hrs for complete combustion (Farook and Muazu 2013). The ash was labeled MHA.

### 2.3. Preparation of sodium silicate

MHA (7.55 g) was dissolved in 500 ml of 3M NaOH in a plastic container. The mixture was stirred for 24 hrs and filtered. On filtration, the deep brown filtrate obtained was taken as sodium silicate solution.

### 2.4. Preparation of SiO<sub>2</sub>/Al/Zn

Al(NO<sub>3</sub>)<sub>3</sub> (8.84 g, 40 mmol) and Zn(NO<sub>3</sub>)<sub>2</sub> (7.84 g, 40 mmol) were dissolved in 176.8 ml distilled water. The mixture was added to 260 ml of 3M HNO<sub>3</sub>. The above mixture was used to titrate sodium silicate obtained from MHA until a pH of 5 when the gel was formed and was aged for 48 hrs. The aged gel was filtered using vacuum filtration apparatus and washed several times with distilled water. The SiO<sub>2</sub>/Al/Zn obtained was dried at 110 °C for 24 hrs (Farook and Muazu, 2013).

### 2.5. Preparation of Adsorbate

The analytical grade adsorbates (methylene blue and malachite green) were used without any further treatment. A 50 mg of the adsorbate was dissolved in 1000 ml of distilled water as stock solution. The methylene blue was labeled MB and malachite green MG (Figure 2).

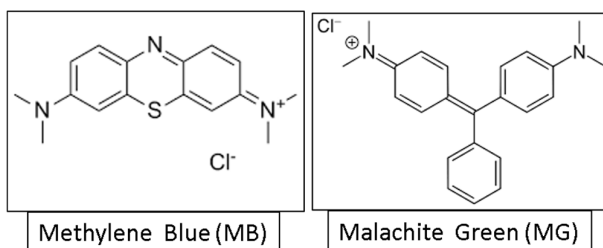


Figure 2: Chemical structures of the adsorbates

### 2.6. Characterization of the Adsorbents

The FT-IR spectra were recorded using VERTEX 70/70V spectrophotometer (Agilent Technologies) within the range of 4000-650 cm<sup>-1</sup>. The Scanning electron microscopy was also carried out using Phenom 800-07334 Scanning Electron Microscope at accelerating voltage of 15 KV, beam size 3.0, working distance 10 and magnification of 1000. Powder X-ray diffraction (PXR) was conducted using a PAN analytical England Philips diffractometer at the central research laboratory, Umaru Musa Yar Adua University, Katsina. The analysis was carried out at room temperature in the range of 5.0 to 70.0 Å electromagnetic spectrum at a scan rate of 12.0 °/min and 0.10 sec integration time. The pH of zero charge (pH<sub>pzc</sub>) characterization of the adsorbent was determined using solid addition method according to Yavena and Geougieva (2014).

### 2.7. Batch Adsorption Experiments

Adsorption of MB and MG on the adsorbent was carried out using batch adsorption method. Various parameters such as contact time, initial dye concentration, adsorbent dosage, pH and adsorption temperatures were studied at constant agitation rate of 200 rpm and room temperature (25 °C) in triplicate and only the average was taken. The adsorption measurements were conducted by mixing various amounts of adsorbents in Erlenmeyer conical flasks (250 ml) containing 50 ml of dye with known concentration. The solutions were

agitated using an orbital shaker for a predetermined time to attain equilibrium after which the samples were taken out and the supernatants were separated from the adsorbent by filtration using Whatman No. 41 filter paper and centrifugation at 100 rpm for 20 minutes. The filtrates were analyzed using UV-Visible spectrophotometer at maximum wavelength ( $\lambda_{max}$ ) of 664 nm for MB and 624 nm for MG dye solution, reporting each data as an average value of triplicate readings. In each case the percentage adsorption (% adsorbed) and equilibrium adsorption capacity,  $q_e$  (mg/g) were evaluated using Equations 1 and 2.

$$\% \text{ adsorbed} = (C_o - C_e)/C_o \times 100 \quad (1)$$

$$q_e = (C_o - C_e)V/W \quad (2)$$

Where  $C_o$  (mg/L) initial dye concentration,  $C_e$  (mg/L) is equilibrium concentration,  $t$  (min) is the time,  $V$  (L) is the volume of the solution used and  $w$  (g) is the mass of the adsorbent used.

### 3. RESULTS AND DISCUSSION

#### 3.1. pH of Zero Charge

Determination of pH of zero charge of adsorbent is important in elucidating adsorption mechanism. Adsorption of cation is favoured at  $pH > pH_{pzc}$  while anion adsorption is favoured at  $pH < pH_{pzc}$ . The surface zero-point charge ( $pH_{pzc}$ ) of the adsorbent was determined and the result is shown in Figure 3. The values of surface zero-point charge ( $pH_{pzc}$ ) of the adsorbent was found to be 8.3. This implied that the adsorbent was alkaline and thus favour the adsorption of cations.

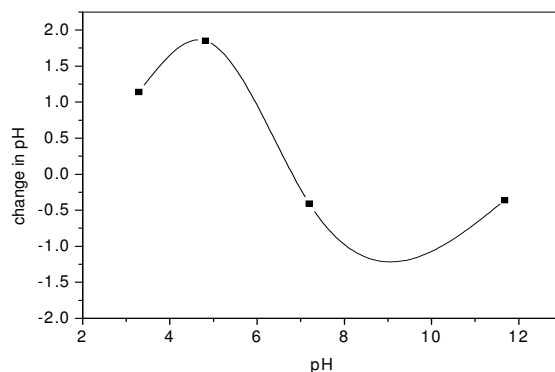


Figure 3: The pH of zero charge of the SiO<sub>2</sub>/Al/Zn

#### 3.2. Batch Adsorption

##### 3.2.1. Effect of contact time

Generally, the rate of removal of dye increases with increasing contact time (Ansari and Mosayebzadeh, 2010). It is clear in the adsorption of MB that the amount of dye uptake was rapid within the first 20 minutes where it shows that the adsorption increased from 94.80 to 95.24% while that of MG increased from 83.63 to 88.75%. However, after 50 minutes, the adsorption of MB did not change significantly, while that of MG dropped significantly to about 86%. This could be associated with blocking of adsorbent pores with saturated molecules of adsorbed MG. Further increase in contact time did not increase the uptake due to desorption of dye on the already occupied adsorption sites (Ansari and Mosayebzadeh, 2010). Figure 4 reveals that the adsorption is rapid in the initial stage and progressed gradually until equilibrium was achieved.

### 3.2.2. Effect of initial dye concentration

The effect of initial dye concentration on the adsorptions of MB and MG dyes on the adsorbent are presented in shown in Figure 5. The experiment was carried out at room temperature using 10-50 mg/L dye concentration for 50 minutes at pH 8.3. From the result, it is observed that the percentage adsorption of MB and MG increases with increasing initial dye concentration from 91.24 to 98.70% and 82.30 to 88.81% for MB and MG respectively. At low dye concentration there is a high availability of adsorption sites and therefore all dye ions bind to the adsorbent. The effect of initial dye concentration depends on the immediate relationship between the concentration of the dye and the available binding sites on the adsorbent surface (Salleh *et al.*, 2011). Normally adsorption of dye is high at lower concentration. However, as the dye concentration increases the level of adsorption also increased probably due to increase in number of available adsorption sites (Bulut and Aydin 2006).

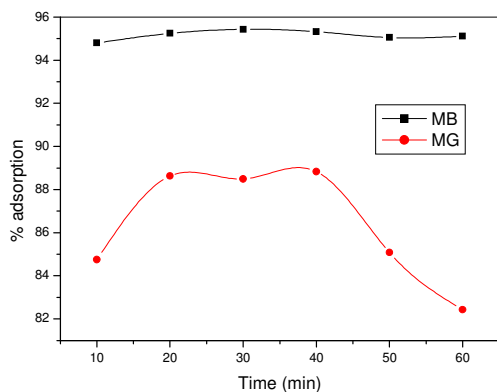


Figure 4: Effect of time on adsorption of MB and MG onto SiO<sub>2</sub>/Al/Zn

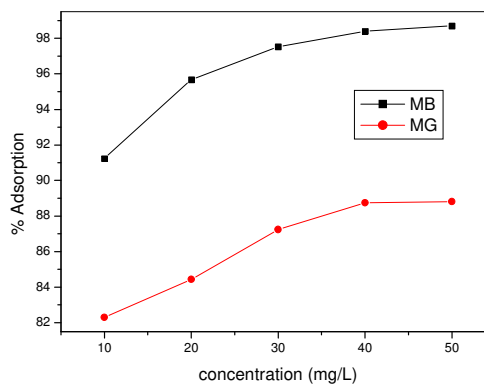


Figure 5: Effect of initial dye concentration on adsorption of MB and MG onto SiO<sub>2</sub>/Al/Zn

### 3.2.3. Effect of adsorbent dose

The effect of adsorbent dose on the adsorption of MB and MG is shown in Figure 6. The effect was studied at room temperature using 0.5–2.5 g adsorbent dosage, 10 mg/L adsorbate concentrations for 30 min at pH of 6 and 8 for MB and MG respectively. It was observed that as the dose of the adsorbents increased from 0.5 to 1.0 g, the amount of dyes adsorbed from aqueous solution also increased slightly (97.10% to 97.60%) for MB and quite significantly (86.39 to 88.02%) for MG before equilibrium was attained (i.e. from 1.5 to 2.5 g). The number of sites available for the adsorption of dyes is directly proportional to the amount of adsorbent used in the measurement. Therefore, increasing the amount of adsorbent leads to an increase in the number of active sites and therefore to a linear increase in the number of ions adsorbed by the material (Anwar *et al.*, 2010). However, no significant change was observed after a dosage of 1.5 g, suggesting that at this point dyes and adsorption sites have reached equilibrium (Rahmani *et al.*, 2010).

### 3.2.4. Effect of initial dye pH

Studies on the effect of initial dye pH were carried out on MB and MG on the adsorbent. The results are given in Figure 7. The graphs showed the % adsorbed at predetermined times corresponding to different initial dye pH ranging from 2 to 12. Generally, at low pH solution, the percentage dye removal decreases for cationic dyes, while at a high pH the percentage of dye removal increases for cationic dye adsorption (Salleh *et al.*, 2011). Both MB and MG are cationic dyes, thus adsorption at lower pH may not be favoured, probably due to the presence of excess H<sup>+</sup> ions competing with the cation groups on the dye for adsorption (Crini et al, 2007). As surface charge density decreases with an increase in the solution pH, the electrostatic repulsion

between the positively charged dye and the surface of the adsorbent is lowered, which may result in an increase in extent of adsorption (Chen and Wang, 2006). With an increase in pH of the solution, the electrostatic repulsion between the positively charged cationic dyes and the surface of adsorbent is lowered and consequently the removal efficiency is increased (Ansari and Mosayebzadeh, 2010). Figure 7 indicated that, the adsorption of MB increased from 96.31 at pH 2 to the highest point of adsorption of 97.36 at pH 6, and later decreases to 96.71 at pH 10. The adsorption of MG increases from 87.02% at pH 2 to 89.00% at pH 8 and later decreases to 87.64 at pH 12.

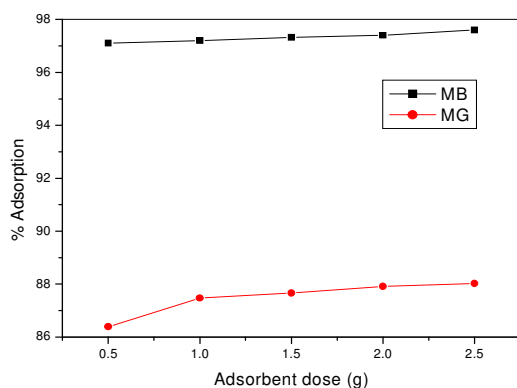


Figure 6: Effect of adsorbent dosage on adsorption of MB and MG onto  $\text{SiO}_2/\text{Al}/\text{Zn}$

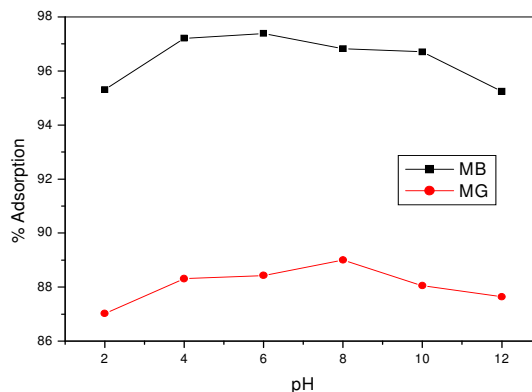


Figure 7: Effect of pH on adsorption of MB and MG onto  $\text{SiO}_2/\text{Al}/\text{Zn}$

### 3.2.5. Desorption efficiency

Desorption studies were performed with 1% HCl,  $\text{H}_2\text{SO}_4$  and NaOH. The result of the desorption studies of the methylene blue and malachite green on the adsorbent were presented in Figure 8a and 8b. NaOH proved to be the best desorption solution with percentage desorption of 75.67% for MB and 74.63% for MG after 30 minutes, this was followed by  $\text{H}_2\text{SO}_4$  with percentage desorption of 35.56% for MB and 33.26% for MG. HCl showed the least desorption solution of the three solutions with 28.48 % for MB and 18.26 % for MG. The result obtained is consistent with that of Pathania et al. (2017) for desorption of MB using activated carbon from *Ficus carica*.

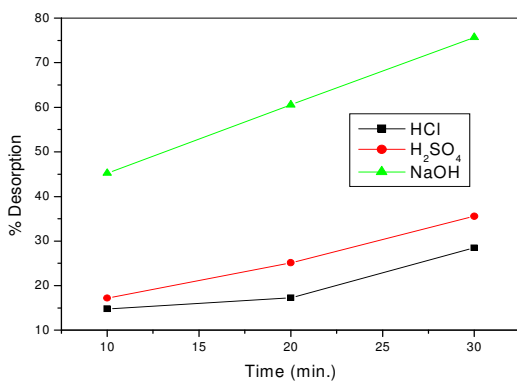


Figure 8a: Percentage desorption of MB using HCl,  $\text{H}_2\text{SO}_4$  and NaOH solutions

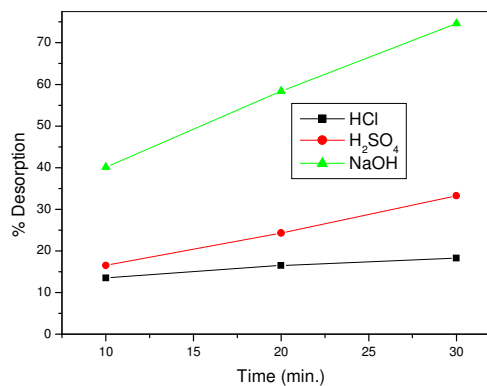


Figure 8b: Percentage desorption of MG using HCl,  $\text{H}_2\text{SO}_4$  and NaOH solutions

### 3.3. Kinetic Study

The results for the adsorption kinetic studies for methylene blue and malachite green on the adsorbent are shown in Table 1. Pseudo first order kinetics was tested for MB and MG adsorption on to the adsorbent. The result of adsorption of MB has high  $R^2$  value of 0.824, while that of MG has  $R^2$  value of 0.956. The adsorptions of both MB and MG do not follow pseudo first order despite high value of  $R^2$ . Also, both  $q_{e,exp}$  (mg/g) and  $q_{e,cal}$  (mg/g) are not in agreement, hence adsorptions of both MB and MG do not follow first order kinetics. This implies that, rate of adsorption of MB depends only on initial concentration of dye or number of adsorbent sites. The pseudo second order kinetics was modeled for methylene blue and malachite green adsorption on the adsorbent. Table 1 shows the pseudo-second order kinetic parameters for MB and MG. The experimental adsorption capacity  $q_e$  (exp) (mg/g) and calculated equilibrium adsorption capacity  $q_e$  (cal) (mg/g) for both MB and MG are in agreement unlike in pseudo first order. The result of adsorptions of MB and MG have high  $R^2$  values of 1 for each of the correlation coefficient  $R^2$ . The adsorptions of MB and MG dyes strongly follow pseudo second order kinetics.

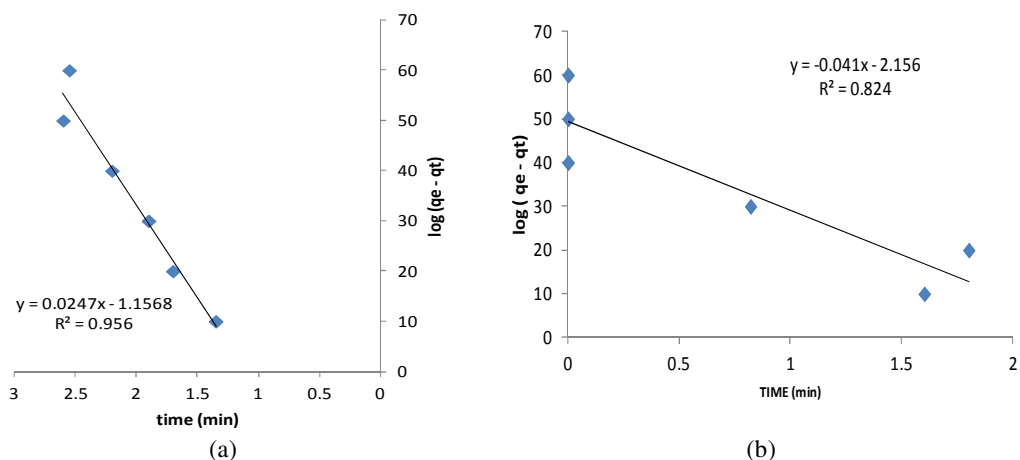


Figure 9: Pseudo first order kinetics for (a) MG and (b) MB

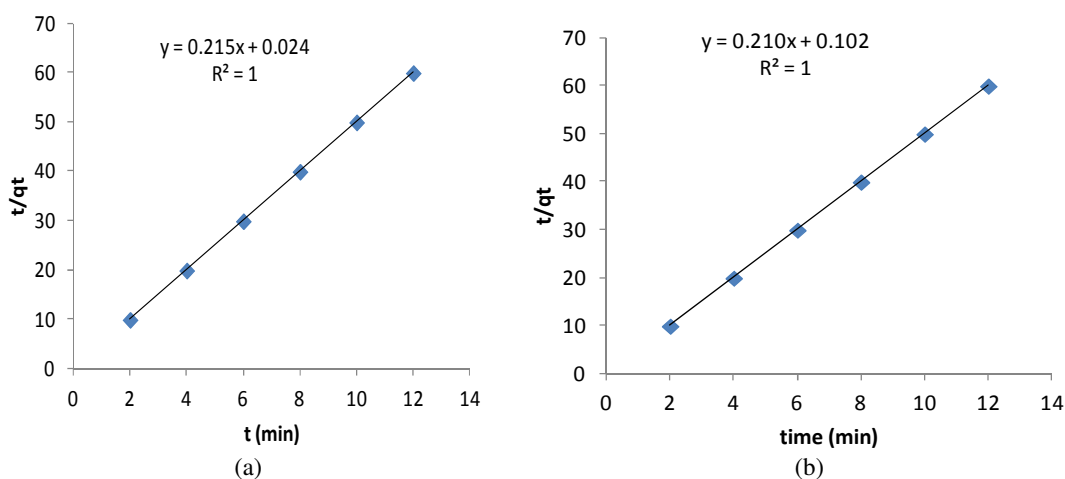


Figure 10: Pseudo second order kinetics for (a) MG and (b) MB

Table 1: Kinetic models

Kinetic models	Constants	MB	MG
Pseudo first order	$q_{e(\text{exp})}$ mg/g	4.572	4.639
	$q_{e(\text{cal})}$ mg/g	143.219	14.322
	$K_1$ min <sup>-1</sup>	0.0944	0.0553
	$R^2$	0.824	0.957
Pseudo second order	$q_{e(\text{exp})}$ mg/g	4.572	4.639
	$q_{e(\text{cal})}$ mg/g	4.762	4.651
	$K_2$ gmin <sup>-1</sup> mg <sup>-1</sup>	0.4323	1.9262
	$R^2$	1	1

As described by Qin et al. (2009), the adsorption of MB and MG through pseudo second order kinetics implies that the rate limiting step during adsorption is based on chemisorption. In this case, the formation of intermolecular interaction between MB and MG dye molecules and adsorption sites through van der Waal forces, electrostatic forces and hydrogen bonds is the key to the adsorption. Therefore, the rate of MB and MG adsorptions were dependent on both concentration of dye molecules and surface characteristics of the adsorbent.

### 3.4. Adsorption Isotherms

The results for the adsorption isotherm studies for the adsorbents are presented in Table 2 showing the values for the adsorption isotherm constants corresponding to the adsorptions of methylene blue (MB) and malachite green (MG) dyes.

#### 3.4.1. Langmuir adsorption isotherm

The Langmuir isotherm is used to determine whether the adsorption process occurs through monolayer formation. Langmuir isotherm model was tested on the adsorption of MB and MG on the adsorbent and the results were presented in Table 2, Figure 11 (a) and (b) respectively. Results showed the adsorption of MB and MG followed Langmuir isotherm for having high  $R^2$  values of 0.997 and 0.998 respectively. Higher values for the regression coefficient,  $R^2$  confirmed that the adsorption followed the Langmuir model.

#### 3.4.2. Freundlich isotherm

The Freundlich isotherm model was tested on the adsorption of MG and MB on the adsorbent and the result were presented in Table 2, Figure 12 (a) and (b) respectively. The Freundlich isotherm assumes that dye uptake occurs on heterogeneous surface by multilayer adsorption and the amount of adsorbate adsorbed increases infinitely with an increase in solute concentration. The  $R^2$  values for the adsorption of MG and MB are both 0.999. The  $K_F$  values for the adsorption of MB and MG were about 42 and 44 respectively. Higher value of  $K_F$  indicate easy uptake of dye from the solution.

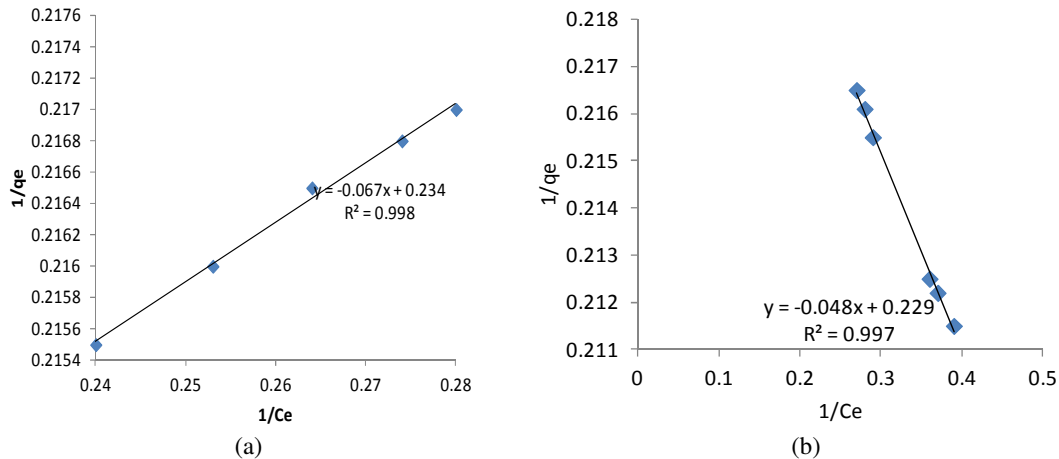


Figure 11: Langmuir isotherm plot for (a) MG and (b) for MB

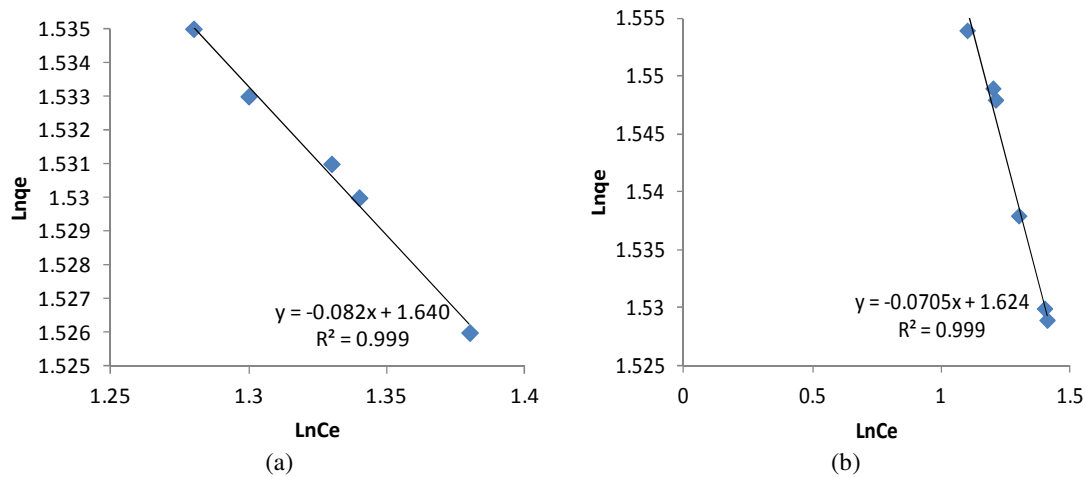


Figure 12: Freundlich isotherm plot for (a) MG and (b) for MB

Table 2: Adsorption isotherm

Isotherm Parameters	Constants	MB	MG
Langmuir	$q_m(\text{mg/g})$	20.833	14.925
	$K_L$	0.209	0.286
	$R_L$	0.229	0.234
	$R^2$	0.997	0.998
Freundlich	$ \ln $	14.286	12.195
	$K_F$	42.073	43.651
	$R^2$	0.999	0.999

### 3.5. Scanning Electron Microscopy (SEM)

The surface morphologies of the adsorbent at different magnifications are shown in Figure 13 which revealed that the surface morphology of the adsorbent has no expanded cavities with irregular pores.

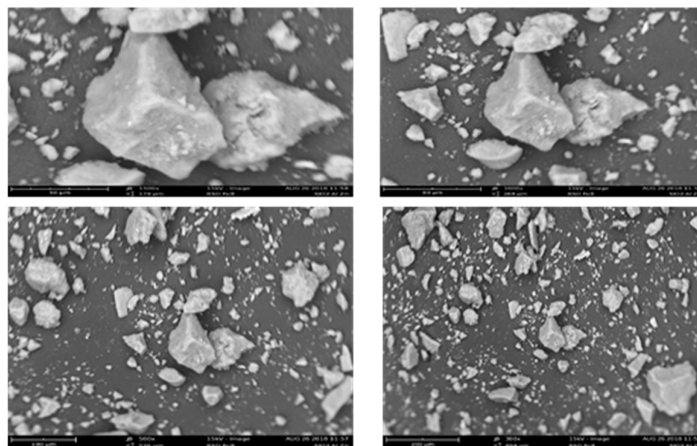


Figure 13: SEM images of fresh SiO<sub>2</sub>/Al/Zn at different magnification

### 3.6. Fourier Transform Infrared (FTIR) Spectroscopy

The result of FT-IR spectra of the adsorbent before and after adsorption with MB and MG is shown in Figure 14. The FTIR analysis of SiO<sub>2</sub>/Al/Zn was carried out between 10,000-0 cm<sup>-1</sup> to determine the vibrational frequency changes in the functional groups in the adsorbent after adsorption. The peak at 698 cm<sup>-1</sup> in the spectra after adsorption with MB can be assigned to the bending modes of aromatic compounds. The additional peaks and changes in the vibrational frequencies after adsorption of dyes indicates that adsorption has taken place (Bharathi and Ramesh, 2013). The blue and orange colours in the figure show that the spectra before and after adsorption of both MB and MG are different.

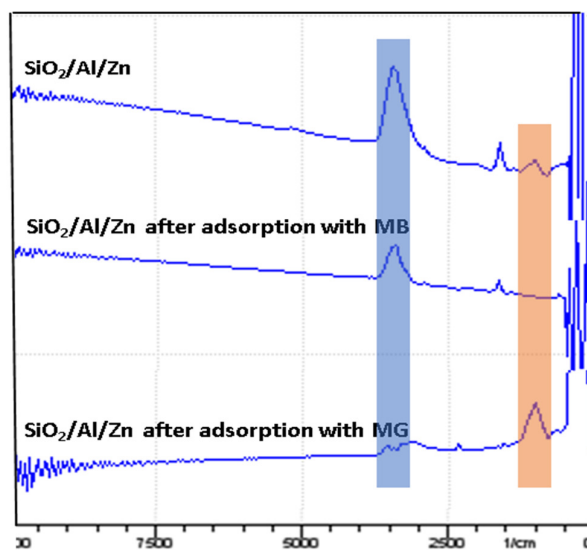


Figure 14: FT-IR spectra of the adsorbent and adsorbent-adsorbate

### 3.7. XRF Analysis

The XRF revealed that there was formation of the SiO<sub>2</sub>/Al/Zn adsorbent. Among all the elements tested for, it is obvious that the concentrations of Al, Si and Zn which were; 38700, 84941 and 33280 respectively were

significantly higher than other elements as shown in Table 3. This confirmed that the adsorbent SiO<sub>2</sub>/Al/Zn was successfully prepared.

Table 3: Analyte concentration as shown by XRF Analysis

Element	Concentration (wt %)
Mg	0.03
Al	3.87
Fe	0.03
Si	8.49
Zn	3.33
Ni	0.05

#### 4. CONCLUSION

Silica supported Aluminium Zinc (SiO<sub>2</sub>/Al/Zn) has been successfully prepared as adsorbent, as revealed by the results of complementary techniques such as FT-IR, XRF and SEM. Subsequently, the prepared silica supported Al/Zn adsorbent was tested for the removal of methylene blue and malachite green from aqueous solution. The optimum contact time to attain equilibrium was 40 minutes for MB and 50 minutes for MG. Similarly, there was an increase in adsorption with increasing initial dye concentration, probably due to increase in number of available adsorption sites. As the adsorbent dose increases, the percentage adsorption also increased, and this could be attributed to the presence of free available sites. The percentage adsorption strongly depends on the pH of the dye solution. The kinetics of the adsorption process follows a pseudo second order law. Langmuir and Freundlich were used to describe the adsorption isotherm and the data obtained fitted the two models. The study also reveals that the prepared adsorbent adsorbs more of methylene blue than malachite green at the same maximum concentration. In conclusion the findings suggest that agricultural wastes e.g. millet husk can be used as a better and low-priced adsorbent for adsorption of dyes.

#### 5. ACKNOWLEDGEMENT

The authors would like to thank Umaru Musa Yaradua University, Katsina and Tertiary Education Trust Fund for partly sponsoring this research.

#### 6. CONFLICT OF INTEREST

There is no conflict of interest associated with this work.

#### REFERENCES

- Anwar, J., Shafique, U. Waheed, Z., Salman, M., Dar, A. and Anwar, S. (2010). *Bioresource Technology*. 101, pp. 1752
- Ansari, R., Mosayebzadeh, Z. (2010), Removal of basic dye methylene blue from aqueous solutions using sawdust and sawdust coated with polypyrrole, *Journal of the Iranian Chemical Society*, 2(7), pp. 339-350
- Bharathi, K. S., Ramesh, S. T. (2013). Equilibrium, thermodynamic and kinetic studies on adsorption of a basic dye by *Citrullus lanatus* rind. *Iran Journal Energy of Environment* 3 (1), pp. 23-34.
- Bulut, Y. and Aydin H (2006) A kinetics and thermodynamics study of methylene blue adsorption on wheat shells, *Desalination* 194 (1-3), pp. 259-267.
- Carneiro, P. A., Umbezeiro, G. A., Oliveira, D. P., Zanoni, M. B. P. (2010). Assessment of water contamination caused by mutagenic textile effluents/dye house effluents bearing dispersed dyes. *Journal of Hazardous Materials*, 174, pp. 694-699.

- Chatterjee, S., Chatterjee, B. P., Guha, A. K. (2007). Adsorptive removal of congo red, a carcinogenic textile dye using hydrobeads: Binding mechanism, equilibrium and kinetics; *Colloids and surfaces A: Physicochemical and Engineering aspects*, 299 (1-3), pp.146-152.
- Chen C. and Wang X. (2006) Adsorption of Ni(II) ions from aqueous solution using oxidized multiwall carbon nanotubes. *Industrial and Engineering Chemical Research* 45(26), pp. 9144-9149
- Crini G., Peindy H.N., Gimbert F. and Robert C. (2007). Removal of C.I Basic Green 4 (malachite green) from aqueous solution by adsorption using cyclodextrin-based adsorbent: Kinetic and equilibrium studies. *Separation and Purification Technology*. 53 (1) pp. 97-110
- Das, A. Subramanyam, B. (2009) Linearised and non-linearised isotherms comparative study on adsorption of aqueous phenol solution in soil; *International Journal of Environmental Science & Technology* 6 (4), pp. 633-640.
- Farooq, A. and Muazu, S. B. (2013). The tetramethylguanidine –silica nanoparticle as an efficient and reusable catalyst for the synthesis of cyclic carbonate from carbon dioxide and propylene carbonate. *Applied catalysis A: general*, 454, pp.164-171.
- Jimoh, R. A., Banuso, O., Rasheed, T., Oyelessa, F., Mosirade, W. (2013). Exploratory assessment of strengths characteristics of millet husk ash (MHA) blended cement laterized concrete. *Advances in Applied Science Research* 4(1), pp. 452-457.
- Khaled, A., Nemr, A. E., El-Sikaily, A. and Abdulwahab, O. (2009). Removal of Direct N Blue 106 from artificial textile dyes effluent using activated carbon from orange peel. *Journal of hazardous materials*, 165(1-3), pp. 100-110.
- Kurniawan, T. A., Chan, G.Y.S. Lo, W.H. and Babel, S. (2006). Comparison of low-cost adsorbents for treating wastewaters laden with heavy metals. *Science of Total Environment*, 366, pp. 409-426.
- Olgun, A. and Atar, N. (2012). Equilibrium, thermodynamic and kinetic studies for the adsorption of lead (II) and nickel (II) onto clay mixture containing boron impurity. *Journal of Industrial and Engineering Chemistry Research*, 18, pp. 1751-1757.
- Pathania, D., Sharma, S. and Singh, P. (2017) removal of methylene blue by adsorption on to activated carbon developed from *Ficus Carica* blast. *Arabian journal of chemistry*, 10, pp. S1445-S 1451
- Ponnusami, V., Vikiram, S. and Srivastava, S. N. (2010). Guava leaf (*Psidium guajava*) powder novel adsorbent for removal of methylene blue from aqueous solutions. *Journal of Hazard Materials*, 152, pp. 276-286.
- Qin, Q. D., Ma, J. and Liu, K. (2009). Adsorption of anionic dyes on ammonium-functionalized MCM-41. *Journal of Hazardous Materials*, 162, pp. 133-139.
- Rahmani, A., Mousavi, H.Z. and Fazli, M. (2010). Effect of Nanostructure Alumina on Adsorption of Heavy Metals. *Desalination*, 253, pp. 94-100.
- Salleh, M.A., Mahmud D.K., Abdul Karim W.A and Idris A (2011). Cationic and anionic dye desorption by agricultural solid waste: A comprehensive review. *Desalination* 280 (1-3), pp. 1-13
- Solfes, E. J. (2000). Thermochemical routes to local fuel and energy from forestry and agricultural residues. 4<sup>th</sup> edition. Plan Press, New York, pp. 23-47.
- Yavena, Z and Geougieva (2014). Study on the physical chemistry. Equilibrium and kinetic mechanism of biosorption by *Zea mays* biomass. *Journal of dispersion science and technology* 35(2), pp. 193-204.